Analytical Methods

ROYAL SOCIETY OF CHEMISTRY

COMMUNICATION

View Article Online
View Journal | View Issue

Cite this: *Anal. Methods*, 2025, **17**, 8115

Received 28th July 2025
Accepted 30th September 2025

DOI: 10.1039/d5ay01249j

rsc.li/methods

Non-destructive colorimetric detection of milk freshness by starch–alginate sensor beads stabilized by nanoemulsions†

E. Aswathy and Lisa Sreejith *

The study presents the development of Ca^{2+}-crosslinked starch–alginate beads encapsulating ternatin-loaded nanoemulsions (SAB) for rapid detection of milk spoilage. The beads exhibited strong, stable colorimetric responses ($\Delta E > 50$) across the pH range (5–7), shifting from light blue in fresh milk, dark blue in spoiling milk and blue-grey in spoiled milk. Encapsulation of the nanoemulsion within the bead effectively prevented the leaching of ternatin, while structural integrity was confirmed by FTIR and TGA analyses. Dry SAB showed superior stability in liquids and 87% cell viability, confirming its non-toxic nature. Unlike conventional techniques, SAB enabled fast, non-destructive on-site spoilage monitoring, highlighting its potential for real-time food safety applications.

Fresh milk (pH 6.5–6.8) is a nutrient-rich medium highly susceptible to microbial contamination. Pathogenic species pose health risks, while spoilage microorganisms and their enzymes rapidly degrade proteins, fats, and sugars, leading to acidification, rancidity, off-flavors, and reduced shelf life, even under refrigeration or pasteurization.[1] Several detection techniques, including ELISA, PCR, ATP sensors, wireless RFID sensors, and electronic noses,[2] have been explored (Table S.1, SI). However, routine monitoring of spoilage still relies on pH measurements because of their simplicity and cost-effectiveness.

Synthetic pH indicators such as methyl red, bromothymol blue,[3] cresol red,[4] and bromocresol green[5] provide distinct color changes during milk spoilage. Yet, their non-biodegradable nature, potential toxicity, and incompatibility with bulk food monitoring limit practical use. For example, methyl red causes acute oral and dermal toxicity and respiratory tract irritation,[6] while bromothymol blue and methylene blue, though less harmful at low concentrations, can disrupt cellular activity and cause adverse health effects at higher levels.[7] To mitigate such concerns, natural halochromic indicators derived from black carrot,[8] blueberry,[9,10] açaí,[11] jaman,[12] and mulberry[13] have been investigated. Nevertheless, these anthocyanin-based sensors generally exhibit weak colorimetric responses ($\Delta E < 20$), poor stability above pH 5, and leaching into milk,[14,15] compromising analytical reliability.

To address these shortcomings, this study introduces ternatins, a distinct class of polyacylated anthocyanins from butterfly pea (*Clitoria ternatea*) flowers (Table S.2, SI). Their structural stability confers a longer shelf life at neutral pH compared to most anthocyanins,[16] making ternatins practical for monitoring milk freshness. Unlike conventional anthocyanins, ternatins exhibit superior thermal stability (up to 70 °C), good storage stability at ambient temperature,[17] and strong halochromic responses within the range of milk spoilage (pH 5–7). Their antimicrobial and antioxidant properties further enhance their suitability for food applications.[18] However, when incorporated into hydrophilic polysaccharide matrices such as starch and alginate, ternatins show excessive leaching, even after crosslinking.

For the first time, this limitation was addressed by impregnating ternatins into oil-in-water (O/W) nanoemulsions of coconut oil, glycerol monostearate (GM), and cetyltrimethylammonium bromide (CTAB), followed by their encapsulation within a Ca^{2+}-crosslinked starch/alginate shell. The resulting sensor beads (SAB) were stable, leach-proof, and capable of producing strong, reproducible colorimetric responses without contaminating the milk.

Butterfly pea flowers were collected locally. Ethanol (CAS 64-17-5, API grade), sodium alginate (CAS 9005-38-3, food grade), glycerol monostearate 40–55 (GM), and cetyltrimethylammonium bromide (CTAB, CAS 57-09-0) were purchased from Merck Life Science Pvt. Ltd, while coconut (*Cocos nucifera*) oil was obtained from the local market.

A 40 w/v% suspension of butterfly pea petals in 60% ethanol was stirred for 2–3 h at 250–300 rpm. The resulting deep-blue extract was filtered, concentrated using a rotary evaporator,

Soft Materials Research Laboratory, Department of Chemistry, National Institute of Technology Calicut, Kerala, India, 673601. E-mail: lisa@nitc.ac.in

† Dedicated to my mentor, Professor Kabir-ud-Din, Department of Chemistry, Aligarh Muslim University, Aligarh, UP, on his 80th birthday.

Table 1 Sensitivity of BPE (0.1 w/v%) towards 0.1 M buffer solutions at the spoilage pH of milk. Data: average ± SD, $n = 3$, using Microsoft Excel 2019; statistical analysis using Jamovi software: Shapiro–Wilk test: $1 > p > 0.1$; Tukey's HSD test: ($p < 0.05$), effect size >1 (for alphabetical notation)

Color parameters	Blank	pH			
		5	6	6.5	7
R	117.45 ± 10.58[a]	87.28 ± 3.99[b]	105.00 ± 7.84[a]	160.63 ± 9.02[c]	104.73 ± 10.07[a]
G	164.82 ± 34.00[a]	115.71 ± 2.87[b]	172.91 ± 7.05[a]	208.18 ± 7.85[a]	170.00 ± 9.07[a]
B	203.09 ± 10.98[a]	169.14 ± 3.08[b]	189.18 ± 7.41[a]	229.27 ± 7.43[c]	187.91 ± 9.92[a]
ΔE	—	—	63.14 ± 9.78[a]	77.12 ± 4.26[a]	79.34 ± 7.74[a]
Color					

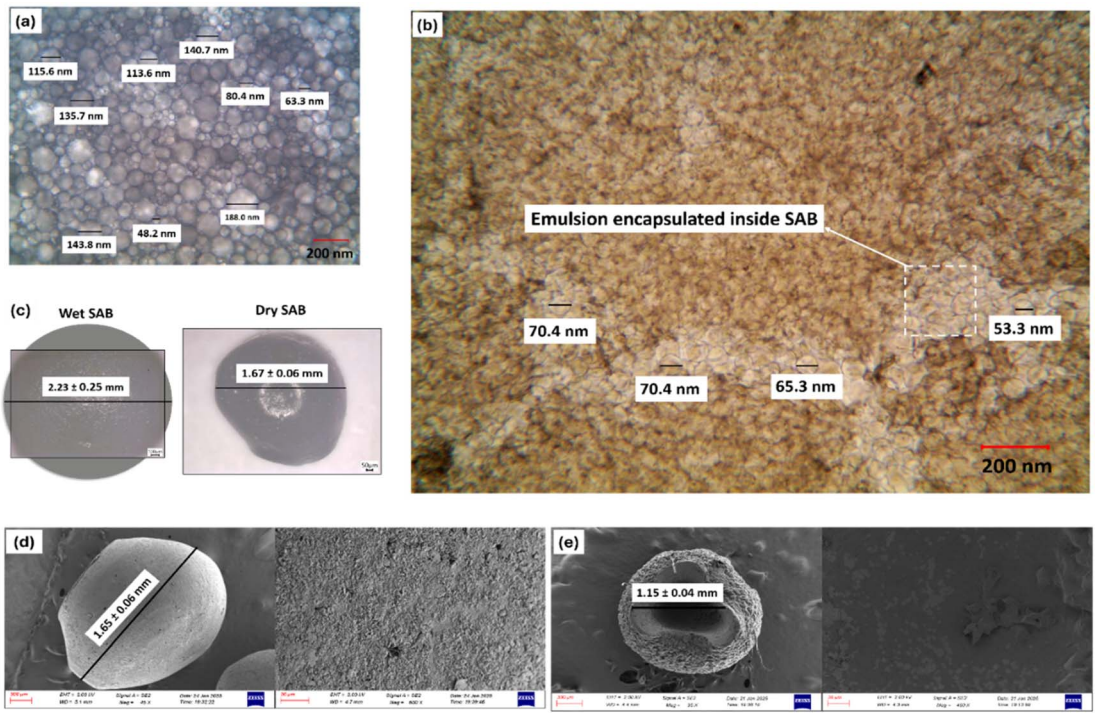

Fig. 1 Phase contrast microscopic images of (a) O/W microemulsion containing BPE and (b) ruptured beads of wet SAB. (c) Optical microscopic images of SAB in both wet and dry forms. SEM images of dry SAB and its surface when washed with (d) distilled water and (e) acetone, generated by capturing secondary electrons at an acceleration voltage of 20 kV.

dried in a hot-air oven at 50 ± 5 °C, and stored in an airtight container under cool, dry conditions.

The absorption spectrum of 0.1 w/v% aqueous butterfly pea extract (BPE) showed four characteristic bands corresponding to polyacylated anthocyanins (290–300 nm), flavylium cation (540 nm), neutral quinonoid base (570–575 nm), and anionic quinonoid base (590–620 nm).[19] Variation in the intensity of these bands determined the color response of BPE across pH buffers (Fig. S.1, SI). In the pH range 5–7, which corresponds to milk spoilage, BPE exhibited a distinct transition from dark blue to cyan due to changes in the relative concentrations of neutral and anionic quinonoid base forms of ternatins[20] (Fig. S.2, SI and Table 1).

A solution was prepared by adding 0.18 g glycerol monostearate (GM) to 1 g coconut oil and heating at 40 °C until clear. To this, 0.01 g BPE, 8.3 mL distilled water, and 0.5 g cetyltrimethylammonium bromide (CTAB) were added, stirred, and stored in a 15 mL airtight vial at 4 °C for 30 min. The non-ionic surfactant GM facilitated the formation of oil-in-water (O/W) emulsion,[21] while the cationic surfactant CTAB promoted the stabilization of the indicator-loaded nanoemulsion,[22] Fig. 1(a).

Separately, 0.86 g starch and 0.21 g sodium alginate[23] were dispersed in 20 mL distilled water, stirred at 60 °C for 30 min, and cooled to room temperature. To this gelatinized mixture, 0.01 g BPE and 0.2 g calcium chloride were introduced in 9.79 mL distilled water. Although starch and alginate allow high indicator loading, their hydrophilicity often results in excessive ternatin leaching into milk, even after crosslinking.[24] To mitigate this, the gelatinized mixture was instead added dropwise to 10 g of the O/W nanoemulsion containing the indicator and 0.2 g calcium chloride. Excess CTAB in the system induced the

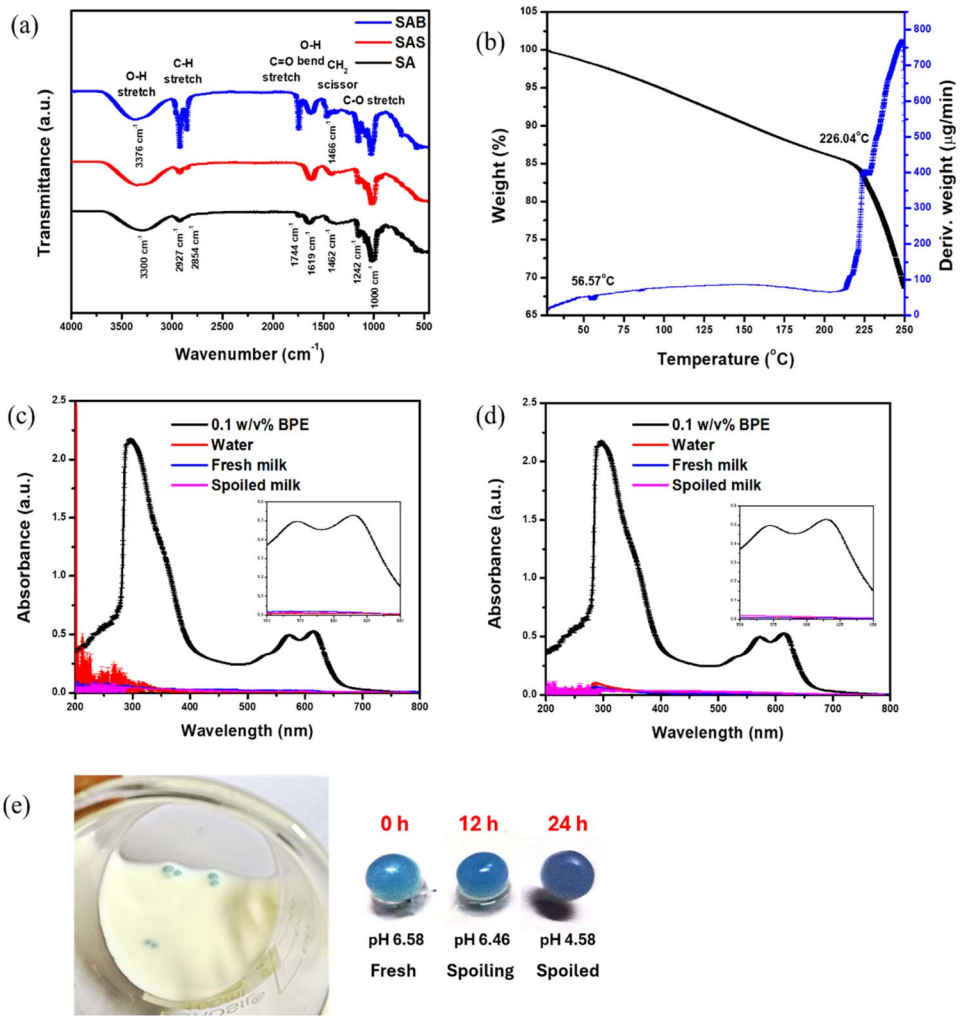

Fig. 2 (a) FTIR-ATR spectra of SA, SAS, and SAB (scan rate: 16 scans per 19 s; spatial resolution: 4.0 cm^{-1}); (b) thermogram and derivative thermogram of dry SAB (obtained from TGA; heating rate: 10 °C min^{-1}; accuracy: ± 0.1 °C; N_2 flow: 200 mL min^{-1}; reference: alumina); comparison of absorption spectra of leachates of (c) wet and (d) dry SAB with that of 0.1 w/v% BPE solution; (e) colorimetric response of SAB to cow milk at an interval of 12 h during its storage at room temperature. Data plotted with average ± SD, $n = 3$, using Origin Pro 8.1 software.

formation of starch–alginate shells that encapsulated the nanoemulsion, yielding stable sensor beads.[25]

Microscopic examination of ruptured wet SAB confirmed the presence of encapsulated nanoemulsions, with droplet sizes ranging from 40–190 nm oozing out of the starch-based shell, Fig. 1(b). The wet beads were dried in a hot-air oven at 50 ± 5 °C for 24 h and equilibrated at 75% RH for 48 h, yielding dry SAB (Fig. S.4, SI). The resulting beads were firm, easy to handle, and required only partial contact with milk, allowing convenient retrieval after freshness monitoring.

As shown in Fig. 1(c), dry SAB displayed a slight surface indentation compared to wet SAB, attributed to moisture loss during drying. Furthermore, Fig. 1(d and e) highlights the distinct surface morphology of dry SAB, with a coarse exterior resulting from Ca^{2+}-mediated crosslinking, and a smooth, non-porous interior encapsulating the nanoemulsion.

The FTIR-ATR spectra (Fig. 2(a)) show a shift in the O–H stretching peak of the Ca^{2+}-crosslinked starch–alginate bead (SA) from 3300 cm^{-1} to 3376 cm^{-1} in the starch–alginate–surfactant (CTAB) hollow bead (SAS),[26] indicating stronger intermolecular hydrogen bonding. The C=O stretching peak at 1744 cm^{-1} confirms the presence of fatty acids in SAB.[27] The O–H bending peak at 1619 cm^{-1} was masked by the aromatic C=C stretching vibration at 1642 cm^{-1} in SAB, evidencing ternatin incorporation.[28,29] Peaks corresponding to $-CH_2$ scissoring and $-CH_3$ bending vibrations of CTAB[30] shifted from 1462 cm^{-1} and 1363 cm^{-1} to 1466 cm^{-1} and 1378 cm^{-1}, respectively, upon nanoemulsion encapsulation, highlighting CTAB's role in both hollow bead and nanoemulsion formation. The bands observed at 1250–1000 cm^{-1} and 1000–700 cm^{-1} correspond to C–O–C stretching of glycosidic linkages and ring vibrations, confirming the presence of polysaccharides such as starch and alginate.[31–33] TGA of dry SAB [Fig. 2(b)] exhibited a distinct degradation peak at 226 °C, attributed to oil,[27] validating the proposed bead structure.

Table 2 Colorimetric response of SAB beads towards cow milk at room temperature for different time durations. Data: average ± SD, $n = 3$, using Microsoft Excel 2019; statistical analysis using Jamovi software: Shapiro–Wilk test: $1 > p > 0.1$; Tukey's HSD test: ($p < 0.05$), effect size >1 (for alphabetical notation)

Properties		Storage time (h)		
		0	12	24
pH		6.58	6.46	4.58
Color parameters	R	73.50 ± 0.71[a]	44.17 ± 5.04[b]	60.67 ± 3.56[c]
	G	147.33 ± 3.27[a]	110.17 ± 3.49[b]	84.33 ± 5.57[c]
	B	205.33 ± 4.75[a]	173.00 ± 4.56[a]	126.67 ± 5.75[c]
	ΔE	—	54.82 ± 4.29[a]	55.56 ± 3.39[b]
	Color			

Dry SAB absorbed ~4.5 times its weight in water to reach the mass of wet SAB. However, its solubility (29%) was markedly lower than that of wet SAB (87%). Despite this, the residual moisture content (5.46%) in dry SAB supports the presence of a W/O emulsion within the dry bead, accounting for its enhanced stability in aqueous environments (Table S.3, SI).

Table 2 illustrates the colorimetric response of the beads, with a variation of $\Delta E > 50$. The beads appeared light blue in fresh milk (pH > 6.5), dark blue in spoiling milk (pH < 6.5), and blue-grey in spoiled milk (pH < 5). The prominent blue hue that appears during acidification corresponds to the accumulation of lactic acid, fatty acids, and amino acids from the breakdown of lactose, milk fats and casein, respectively. At neutral pH, the anionic quinonoid base form of ternatin imparts a cyan hue,[16] responsible for the lighter bead color in fresh milk. As acidity increases, the anionic quinonoid base converts to its neutral counterpart,[16,19] imparting a darker blue hue to the bead, providing a clear visual indication of spoilage (Fig. S.5, SI).

Absorption spectra of bead leachates in distilled water, fresh milk, and spoiled milk showed no peaks at 571 nm and 615 nm (wavelengths characteristic of the neutral and anionic quinonoid base forms of ternatin at pH 5–7), confirming stable encapsulation of the indicator even after extended exposure to liquid analytes. Cytotoxicity assay of dry SABs, quantified by MTT assay (Section S.1.4, SI), demonstrated a cell viability of 87% for 1 h incubation (see Fig. S.6, SI), establishing the non-toxic nature of the technique.

In summary, we developed Ca^{2+}-crosslinked starch–alginate beads encapsulating ternatin-loaded nanoemulsions (SAB) for milk spoilage detection. Both wet and dry SAB were comprehensively assessed for functionality and storage stability, with dry SAB showing superior robustness in liquid analytes. Unlike conventional methods, which require both time and specialized instrumentation, SAB provides rapid, on-site spoilage detection through a distinct color change visible to the naked eye. Notably, SAB avoids indicator leaching and weak colorimetric responses common in the existing systems, instead exhibiting a pronounced ΔE without contaminating the milk. These findings highlight the potential of integrating Dry SAB into storage vessels with engineered caps for real-time monitoring of milk freshness, advancing both food safety and environmental sustainability.

Author contributions

E. Aswathy: writing – original draft, methodology, investigation, formal analysis, visualization, validation. Lisa Sreejith: writing – review & editing, supervision, conceptualization, methodology, resources, project administration, visualization, validation.

Conflicts of interest

There are no conflicts to declare.

Data availability

The data supporting this article have been included as part of the supplementary information (SI). Supplementary information: experimental techniques used in the characterization of SAB, equations used for data analysis, along with certain figures and tables supporting the results. See DOI: **https://doi.org/10.1039/d5ay01249j**.

Notes and references

1 A. Farid, Z. Wang, M. U. Khan, P. Wang, H. Wang, H. Liu and Z. Chen, *Food Microbiol.*, 2025, **130**, 104763.
2 A. Poghossian, H. Geissler and M. J. Schöning, *Biosens. Bioelectron.*, 2019, **140**, 111272.
3 A. Romero, J. L. Sharp, P. L. Dawson, D. Darby and K. Cooksey, *Food Packag. Shelf Life*, 2021, **30**, 100720.
4 I. Molnár-Perl, M. Pintér-Szakács and D. Medzihradszky, *Food Chem.*, 1990, **35**, 69–80.
5 R. Mo, Q. Quan, T. Li, Q. Yuan, T. Su, X. Yan, Z. J. Qian, P. Hong, C. Zhou and C. Li, *ChemistrySelect*, 2017, **2**, 8779–8784.
6 S. Sharma, S. Pathak and K. P. Sharma, *Bull. Environ. Contam. Toxicol.*, 2003, **70**, 753–760.
7 S. Agarwal, H. Sadegh, M. Monajjemi, A. S. Hamdy, G. A. M. Ali, A. O. H. Memar, R. Shahryari-Ghoshekandi, I. Tyagi and V. K. Gupta, *J. Mol. Liq.*, 2016, **218**, 191–197.
8 M. Moazami Goodarzi, M. Moradi, H. Tajik, M. Forough, P. Ezati and B. Kuswandi, *Int. J. Biol. Macromol.*, 2020, **153**, 240–247.
9 R. Gao, H. Hu, T. Shi, Y. Bao, Q. Sun, L. Wang, Y. Ren, W. Jin and L. Yuan, *Curr. Res. Food Sci.*, 2022, **5**, 677–686.

10 D. Chen, J. Lv, A. Wang, H. Yong and J. Liu, *Foods*, 2024, **13**, 2237.
11 S. C. Teixeira, T. V. de Oliveira, L. F. Batista, R. R. A. Silva, M. de P. Lopes, A. R. C. Ribeiro, T. C. B. Rigolon, P. C. Stringheta, N. de and F. F. Soares, *Polysaccharides*, 2022, **3**, 715–727.
12 M. N. Shabbir, A. Ahmad, M. Aslam, A. Hassan, H. Ullah, M. Akram, H. F. Qayum and F. Naeem, *Food Chem.*, 2025, **466**, 142181.
13 S. Wang, S. Liu, X. Yang, S. Zhang, X. Li, L. Zhang and Y. Chen, *Food Biosci.*, 2024, **62**, 105042.
14 M. Cai, C. Xie, H. Zhong, K. Yang and P. Sun, *LWT*, 2021, **144**, 111196.
15 N. I. Wardani, W. Alahmad and P. Varanusupakul, *Handb. Green Anal. Chem.*, 2024, **9**, 100117.
16 G. C. Vidana Gamage, Y. Y. Lim and W. S. Choo, *Front. Plant Sci.*, 2021, **12**, 1–17.
17 N. Turker, S. Aksay and H. I. Ekiz, *J. Agric. Food Chem.*, 2004, **52**, 3807–3813.
18 M. Wang, N. Ji, M. Li, Y. Li, L. Dai, L. Zhou, L. Xiong and Q. Sun, *Food Hydrocolloids*, 2020, **101**, 105565.
19 X. Fu, Q. Wu, J. Wang, Y. Chen, G. Zhu and Z. Zhu, *Molecules*, 2021, **26**, 7000.
20 T. T. Vuong and P. Hongsprabhas, *Cogent Food Agric.*, 2021, **7**, 1889098.
21 M. I. Moran-Valero, V. M. P. Ruiz-Henestrosa and A. M. R. Pilosof, *Colloids Surf., B*, 2017, **151**, 68–75.
22 W. Jiang, W. Xiang, L. Xu, D. Yuan, Z. Gao, B. Hu, Y. Li and Y. Wu, *Food Hydrocolloids*, 2023, **140**, 108607.
23 P. Lertsarawut, S. Laksee, T. Rattanawongwiboon and K. Hemvichian, *Carbohydr. Polym. Technol. Appl.*, 2024, **7**, 100456.
24 L. G. Santos and G. F. Alves-silva, *Int. J. Biol. Macromol.*, 2022, **220**, 866–877.
25 H. Y. Lee, K. R. Tiwari and S. R. Raghavan, *Soft Matter*, 2011, **7**, 3273–3276.
26 Q. Jin, X. Li, Z. Cai, F. Zhang, M. P. Yadav and H. Zhang, *Food Hydrocolloids*, 2017, **70**, 329–344.
27 R. J. Amit, S. Kumari, A. S. Dhaulaniya, B. Balan and D. K. Singh, *LWT*, 2020, **118**, 108754.
28 J. Xiong, Q. Li, Z. Shi and J. Ye, *Food Res. Int.*, 2017, **100**, 858–863.
29 N. A. M. Ghuzali, M. A. A. C. M. Noor, F. A. Zakaria, T. S. Hamidon and M. H. Husin, *Appl. Surf. Sci. Adv.*, 2021, **6**, 100177.
30 G. Su, C. Yang and J. J. Zhu, *Langmuir*, 2015, **31**, 817–823.
31 S. K. Papageorgiou, E. P. Kouvelos, E. P. Favvas, A. A. Sapalidis, G. E. Romanos and F. K. Katsaros, *Carbohydr. Res.*, 2010, **345**, 469–473.
32 R. M. A. Daoub, A. H. Elmubarak, M. Misran, E. A. Hassan and M. E. Osman, *J. Saudi Soc. Agric. Sci.*, 2018, **17**, 241–249.
33 I. Capron, P. Robert, P. Colonna, M. Brogly and V. Planchot, *Carbohydr. Polym.*, 2007, **68**, 249–259.